HHS Public Access
Author manuscript
Soft Matter. Author manuscript; available in PMC 2022 March 11.

Published in final edited form as:
Soft Matter. 2021 March 11; 17(9): 2530–2538. doi:10.1039/d0sm02169e.

Phase Transition Characterization of Poly (oligo (ethylene glycol) methyl ether methacrylate) Brushes using the Quartz Crystal Microbalance with Dissipation

Rohini Thevi Guntnur, **Nicolas Muzzio**, **Madison Morales**, **Gabriela Romero***
Department of Biomedical Engineering and Chemical Engineering, University of Texas at San Antonio, One UTSA Circle, San Antonio, Texas USA 78249

Abstract

Heterogeneous non-linear poly(ethylene glycol) analogs, like poly (oligo (ethylene glycol) methyl ether methacrylate) (POEGMA), are of particular interest in the fabrication of smart biocompatible coatings as they undergo a reversible macromolecular rearrangement in response to external heat stimuli. The phase transition dynamics of POEGMA coatings in response to external temperature stimuli have been poorly investigated. The quartz crystal microbalance with dissipation (QCM-D) can be used to investigate the phase transition of these functional coatings as polymer brushes in a dynamic and noninvasive in situ measurement. POEGMA brushes with different thickness are synthesized from the surface of a QCM-D sensor following a living radical polymerization technique by varying the monomer molecular weight. Investigations on the thermoresponsive collapse and swelling of POEGMA brushes grafted from the surface of a QCM-D sensor reveal the reversible phase transition nature of these coating. Furthermore, the potential of these smart coatings in the field of biotechnology was explored by investigating the absorption and desorption of a model drug. A pulsatile drug release profile triggered by an increase in temperature is observed from POEGMA brushes. POEGMA brushes have the potential to be utilized as polymer coatings for controlled and programable drug release.

Graphical Abstract

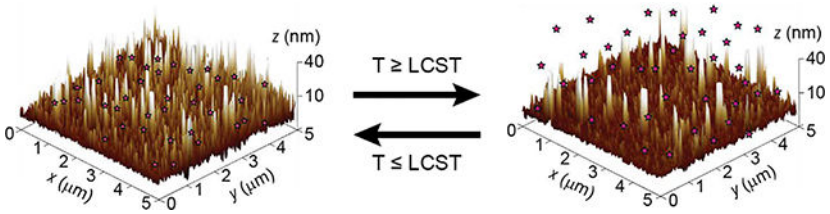

This work investigates the thermodynamic phase transition of poly(oligo(ethylene glycol) methyl ether methacrylate) brushes using the Quartz Crystal Microbalance with Dissipation. Polymer brushes are found to have a reversible phase transition in response to local temperature changes.

*Corresponding author. *Tel. +1 (210) 458 7982*, gabrielaromero.uribe@utsa.edu.

Conflicts of interest
There are no conflicts to declare.
Electronic Supplementary Information (ESI) available: [details of any supplementary information available should be included here].
See DOI: https://doi.org/10.1039/d0sm02169e

Polymer brushes are utilized as smart drug carriers. Drug release from polymer brushes follows a pulsatile profile triggered by the increase of temperature.

1. Introduction

Polymer coatings are widely used in bionanotechnology for many applications, for example to stabilize colloidal particles in biological fluids, where polyethylene glycol (PEG) has been widely exploited [1, 2]. However, new bioapplications require “smart” polymer coatings with multifunctional properties. For instance, synthetic macromolecules undergoing rapid conformational change in response to an external stimulus such as pH, temperature, ionic strength or irradiation are of high scientific interest in biomedical research [3, 4]. Among the temperature responsive polymers, poly(N-isopropylacrylamide) (PNIPAM) is by far the most investigated in materials science, however it has inherent disadvantages for biomedical applications. The presence of multiple amide functional groups in the chemical structure of PNIPAM could lead to the formation of hydrogen bonds with other biopolymers such as proteins [5]. Thus, the synthesis of biocompatible thermo-responsive polymers, such as those composed by oligo (ethylene glycol) macromers, appear to be a promising alternative to conventional PNIPAM.

Oligo (ethylene glycol) macromers are composed of a carbon-carbon backbone and multiple oligo (ethylene glycol) sidechains. Unlike linear PEG, heterogeneous non-linear polymers like poly (oligo (ethylene glycol) methyl ether methacrylate) (POEGMA), undergo to a reversible macromolecular rearrangement in response to external heat [6, 7]. From a physicochemical point of view, the POEGMA comb-shape is singular because its carbon-carbon backbone is hydrophobic while its sidechains are amphiphilic. Modifying the length and chemistry of the side-chains alters hydrophilicity, which can, in turn, influence hydration state and conformation at a given temperature [8]. Additionally, the carbon-carbon main-chain conformation can be directly altered by tuning the length ratio between the main- and side-chains, which influences the sterical repulsions between the side-chains [3, 8]. At low temperature, POEGMA is soluble in water due to the hydration of its sidechains. By increasing temperature, the latter dehydrate, causing polymer collapse, which leads to polymer aggregation and ultimately precipitation. The temperature at which this process begins is referred to as the lower critical solution temperature (LCST). For POEGMA, the collapse process is reversible as there is no strong hydrogen donor in the chemical structure of this polymer, and therefore there is no possibility of forming stable hydrogen bonds in the collapsed state [9].

Phase transition of POEGMA has been thoroughly studied in aqueous solutions, and it has been found that POEGMA LCST is highly dependent on its molecular weight [10–15]. When POEGMA chains are covalently grafted to a surface from one of their sides, the sterical repulsions between neighbouring chains force them to stretch away from the interface forming “polymer brushes” [16]. POEGMA brushes are expected to show similar phase transition behaviours as in solution, however POEGMA brush behaviour has been inextensively studied. POEGMA brushes have been mainly characterized for the thickness of the grafted layer and in less extent for morphological changes at the LCST [17–21]. In this

work, we investigate the phase transition of temperature sensitive POEGMA brushes using the quartz crystal microbalance with dissipation (QCM-D). We synthesize POEGMA brushes with different molecular weight on the surface of a QCM-D sensor by atom transfer radical polymerization (ATRP). Polymer growth and reversible phase transition at the LCST are monitored in real time using QCM-D. Atomic force microscopy (AFM) is used to corroborate polymer brushes topography at the critical transition temperatures. We compare our findings from QCM-D and AFM measurements with structural changes of POEGMA chains in solution to give a greater insight of the phase transitions at the LCST. Additionally, polymer brushes are tested as functional coatings for drug entrapment and release. Drug release kinetics from POEGMA brushes is triggered by the temperature phase transitions. We correlate drug release kinetics with polymer brush thickness.

2. Results and Discussion

Polymer brushes synthesis.

In this work, we proposed QCM-D as a tool to investigate the phase transition of temperature-responsive POEGMA brushes. First, we immobilize a monolayer of the thiol initiator (BBU) on the surface of a gold-coated quartz sensor though silane-gold chemistry (Figure 1a) [22–25]. The QCM-D sensor was incubated overnight with a 10 mM solution of BBU in ethanol. Thiol-end groups of BBU were anchor to the gold surface coating of the QCM-D sensor forming gold-sulphur bonds [26, 27], and leaving the bromide end groups immobilized for further polymerization. Through this method, we were able to immobilize a monolayer of BBU of around 7.5 ± 0.1 nm on the surface of a QCM-D sensor (Figure S2).

POEGMA brushes were synthesized from the BBU-immobilized surface of a QCM-D sensor. Figure 1b depicts the in-situ polymerization of POEGMA brushes using an oligomer with molecular weight of 144 g mol^{-1} (POEGMA-144). The monomer/catalyst mixture was injected into the QCM-D chamber and ATRP was lead for 5 hours. A decrease in the frequency of −45.6 ± 0.1 Hz was observed between the initial water baseline and the last water wash after ATRP. Using Sauerbrey equation, a mass deposition of 4.33 mg cm^{-2} was calculated for POEGMA-144 brushes, which corresponds to a polymer thickness of ~40 nm. Contrary, an increase in the dissipation was observed after ATRP. The increase in dissipation was accompanied by the spread of the harmonics (Figure S3), which corroborates the change in the viscoelasticity of the material being deposited. The slow and steady nature of ATRP reaction was conducted by covering the entire active area of the QCM-D sensor, such as we could safely assume that the mass was evenly distributed. The understanding of rigidity of the grafted polymer brushes and their even distribution over the crystal surface permit for the application of Sauerbrey equation[28].

One way to modify POEGMA brushes thickness is by changing the oligomer size, while maintaining constant ATRP conditions. Following the protocol described above, we also synthesized POEGMA brushes from the surface of QCM-D sensor using oligomers with molecular weights of 188 g mol^{-1} (POEGMA-188) and 300 g mol^{-1} (POEGMA-300) (Figure S4 and S5, respectively). Polymerizations for POEGMA-144, POEGMA-188 and POEGMA-300, were repeated three times each, and the average calculated mass and thickness of the formed brushes are summarized in Table 1. Figure 2 shows polymer brushes

growth as a function of time for the three different oligomers tested (144, 188 and 300). We observed no statistical difference in the thickness of synthesized POEGMA-144 and POEGMA-188 brushes. ATRP polymerization is also known as transition metal-mediated living radical polymerization due to the linear increase in the molecular weight of the polymer showing the "livingness" during the polymerization process [29, 30]. The length and total molecular weight of the synthesized polymer chains depends critically on factors such as monomer ratio, duration of the polymerization reaction, and molecular weight of the monomer. Therefore, one can expect polymer brushes with similar thickness when using oligomers with relatively close molecular weights as is the case for oligomers 144 and 188 g mol^{-1}. For POEGMA-300 brushes, the average calculated thickness was 65 ± 23 nm which is significantly higher than POEGMA-144 or POEGMA-188, confirming that polymer brush thickness depends on the initial molecular weight of the oligomer.

Phase transition of POEGMA brushes.

After POEGMA in situ polymerization by QCM-D, we studied the phase transition of the different POEGMA brushes when subjected to temperature gradients using QCM-D (Figure S6). The temperature in the QCM-D chamber was raised from 24 °C to 65 °C at a rate of 1°C per minute. Then, the temperature was held at 65 °C for 2 minutes to ensure complete collapse of the polymer brushes. Finally, the temperature was brought down from 65 °C to 24 °C at a rate of 1°C per minute and held at 24 °C for 90 minutes to allow complete re-swelling of the brushes. This process was repeated for 10 consecutive cycles. The changes in the frequency and dissipation of a clean gold-plated quartz sensor subjected to the 10 temperature cycles was used as phase transition baseline to ensure that the effects observed were due to the phase transition of the polymer brushes (Figure S7). All the data presented for the phase transition behaviour of POEGMA brushes was normalized by subtracting the phase transition baseline. Figure 3a shows the phase transition behaviour of POEGMA-144 during the 10 temperature cycles followed by QCM-D. As temperature was increased, we observed an increase in the frequency, which indicates mass desorption. As POEGMA-144 collapses with the raise in the temperature, the polymer chains dehydrate and release water, thus the mass desorption. When the temperature was brought down from 65 °C to 24 °C, a decrease in the frequency was observed, indicating absorption of water molecules and POEGMA-144 brushes re-swelling. The dissipation graph provides insight into the changes in the viscoelasticity of the polymer brushes during every stage of the temperature cycle. As temperature increases, dissipation decreases indicating a decrease in the viscoelasticity of the system or the formation of a stiffer coating due to polymer brushes collapse. When temperature decreases back to 24 °C, dissipation increases, indicating an increase in the viscoelasticity or the formation of a softer coating, as it will be the case when polymer brushes are completely swollen. The temperature at which phase transitions were observed by QCM-D for POEGMA-144 was at 42 °C, which is consistent with the LCST of 42 °C previously reported for POEGMA polymers synthesized in solution with an oligomer of 144 g mol^{-1} and similar ATRP conditions [3].

Figure 3b is a compilation of the phase transitions of POEGMA brushes with different thickness (POEGMA-144 and −300) followed by QCM-D. For POEGMA-300 brushes reach higher ΔFrequency values than POEGMA-144 when the local temperature rises.

POEGMA-300 forms longer brushes with higher molecular weight than POEGMA-144, therefore absorb and desorb more water during the temperature cycles. Moreover, POEGMA-300 brushes require more energy to break the hydrogen bonds between the polymer strands and water. The temperature at which phase transitions were observed by QCM-D for POEGMA-300 was at 64 °C, which is consistent with the LCST of 64 °C previously reported for POEGMA polymers synthesized in solution with an oligomer of 300 g mol^{-1} and similar ATRP conditions [3]. Both, POEGMA-144 and POEGMA-300 were responsive to the ten consecutive temperature cycles programmed, showing a reversible phase transition that depends on the LCST. For comparison, we synthesized PNIPAM brushes with a thickness of ~ 35 nm through ATRP from the surface of a QCM-D sensor following the same protocol as for POEGMA brushes. When subjected to the 10 consecutive temperature cycles programmed, we observed only two partial phase transitions for PNIPAM brushes (Figure S8). When the local temperature increases and reaches the LCST of PNIPAM (~ 32 °C), the brushes collapse. When the local temperature decreases following the programmed cycle, PNIPAM brushes undergo phase transition very slowly and do not completely re-swell. During the second increase of temperature, PNIPAM brushes undergo phase transition but they do not completely collapse. When the temperature is decreased in the second cycle, PNIPAM brushes do not recover their original macromolecular arrangement and remained partially collapsed for the next eight temperature cycles. Contrary to POEGMA brushes, PNIPAM brushes are not sensitive to consecutive temperature cycles, suggesting that their thermodynamic phase transition is irreversible or very slow [31, 32].

The effect of temperature and oligomer MW was also investigated by AFM (Figure 4). AFM height image of POEGMA-144 brushes at 25 °C shows a surface covered with protrusions in the range of 15–20 nm height and some higher peaks in the 35–70 nm range (Figure 4a and 4c). These structures become significantly shorter after heating up to 60 °C, with the surface covered with 5–12 nm height protrusions and some of the larger peaks collapsing. The arithmetic average roughness (R_a) also decreased from 5.15 to 3.28 nm when going from 25 to 60 °C. These results are consistent with a phase transition of POEGMA-144 brushes when the temperature is increased above the LCST. AFM height image of POEGMA-300 brushes at 25 °C show higher and wider protrusions in comparison with the ones found on POEGMA-144 brushes (Figure 4b and 4d). The average protrusions range from 30 to 50 nm height with some peaks going far beyond 60 nm. The R_a of the POEGMA-300 brushes is 8.58 nm, a figure larger than that of POEGMA-144 brushes at the same temperature. These data confirm the effect of the initial molecular weight of the oligomer in the polymer brush topography.

Phase transition of POEGMA chains in solution.

POEGMA polymers were further characterized for their phase transition behaviour in their bulk form. POEGMA polymer chains were synthesized by ATRP in solution, unlike polymer brushes that are attached from one end to a surface. Although the ATRP conditions utilized in polymer brush synthesis were replicated for ATRP in solution, the MW of the polymer chains cannot be directly compared. In bulk polymerization it is expected that the initiation and growth will occur more randomized than for polymer brushes, leading to a broader MW distribution. The phase transition of POEGMA chains in solution was studied by measuring

the cloud point temperature through UV-Transmittance. The UV-Transmittance values of POEGMA-144 and POEGMA-300 as a function of temperature are shown in Figure 5a. A clear increase in the transmittance of POEGMA-144 was observed around 42 °C, consistent with previously reported LCST for this polymer and in agreement with the LCST found by QCM-D for POEGM-144 brushes. For POEGMA-300 two increases of transmittance were observed, at 40°C and 57°C, in agreement with previously reported LCST for this polymer and consistent with our findings by QCM-D for POEGMA-300 brushes at a LCST of 64°C. Increase in the UV-transmittance of POEGMA in solution is expected during phase transition due to collapse of the polymer in solution as it gets closer to the LCST, which results in precipitation of the polymer from the solution. This behaviour is known as cloud point temperature and although it is not a direct measure of the LCST it provides a rough representation of the LCST of the polymer in solution [33]. The cloud point temperature of the polymer chains in solution can also be analysed by measuring the hydrodynamic diameter of the polymer aggregates above the critical micellar concentration. Figure 5b shows a drastic decrease in the hydrodynamic size of the POEGMA-144 and POEGMA-300 in solution, confirming that polymer chains undergo conformational changes at their cloud point temperatures measured by UV-Transmittance.

Drug encapsulation and release from POEGMA brushes.

Polymer brushes have been investigated extensively in material science to stabilize colloidal particles and to fabricate smart coatings. For instance, polymer brushes that undergo phase transition upon temperature changes could have potential applications in controlled and programable drug delivery. Moreover, temperature-sensitive PEG analogues such as POEGMA, provide a unique platform for biocompatible smart polymer coatings. We utilize QCM-D to investigate the encapsulation and temperature triggered release of a drug from POEGMA brushes. Capsaicin, a neurostimulator prescribed to manage peripheral nerve pain, was utilized as a model drug. POEGMA-144 brushes grafted from the surface of a QCM-D sensor were incubated with a 0.5 mg mL^{-1} capsaicin solution in 150 mM NaCl for one hour. Following the incubation, the brushes were extensively rinsed with 150 mM NaCl solution to ensure complete removal of unentrapped capsaicin. Through hydrophobic interactions, we were able to encapsulate 60 mg of capsaicin per cm^2 within POEGMA-144 brushes. After capsaicin encapsulation, release kinetics were studied using QCM-D by subjecting POEGMA-144 brushes to the same temperature cycles described before. Figure 6a compares the phase transition of POEGMA-144 brushes with and without capsaicin followed by QCM-D. The difference between the transitions is an indication of additional mass desorption from POEGMA-144 brushes with capsaicin when polymer collapses. The difference in the desorbed mass comprises of the capsaicin and the water molecules released out of the brushes during their conformational change. Capsaicin cumulative release from POEGMA-144 brushes follows a pulsatile profile triggered by the local increase of temperature (Figure 6b). Following the same protocol, capsaicin was also entrapped within POEGMA-300 brushes. Around 517 mg of capsaicin per cm^3 were entrapped within POEGMA-300 brushes. Figure 6c displays the phase transition of POEGMA-300 brushes loaded and unloaded capsaicin followed by QCM-D. We observe a difference between the transitions of POEGMA-300 brushes, suggesting the release of capsaicin and water from the polymer brushes during their conformational change. Figure 6d illustrates the pulsatile

release profile of capsaicin from POEGMA-300 brushes triggered by the local increase of temperature. Capsaicin release from POEGMA-144 and POEGMA-300 brushes followed by QCM-D demonstrates the potential of POEGMA brushes for their application as smart coatings for on-demand controlled drug release triggered by a temperature gradient.

3. Experimental

Materials.

Ethyl alcohol, dimethylformamide (DMF), copper chloride, tetrahydrofuran (THF), 4,4′-dinonyl-2,2′-dipyridyl, oligomers of poly(ethylene glycol) methyl ether methacrylate (POEGMA) with molecular weight: 144, 188 and 300, 11-mercapto-1-undecanol, pyridine, α-bromoisobutyryl bromide, sodium sulphate, potassium chloride were purchased from Sigma Aldrich. Dichloromethane (DCM) was purchased from Alfa Aesar. Triethyoxysilane, Alumina and chloroform-D were purchased from ACROS organics. All chemicals were used with no further purification, with the exception of POEGMA oligomers that were purified through an inhibitor removal column (Sigma Aldrich, cat no. 306312) to increase the reactivity of the chemical. Millipore water from Thermo scientific barnstead SMART2PURE UV/UF water filter was used for experiments. Gold plated QCM-D crystals were purchased from Nanoscience Instruments (QSM 301).

Initiator synthesis.

2-(2-Bromoisobutyryloxy) undecyl thiol (BBU) was used as ATRP initiator in this study. The synthesis was adapted from previously reported protocol [34]. Briefly, BBU was synthesized by adding α-bromoisobutyryl bromide (97.89 mmol) dropwise into a cold solution (0 °C) made of 11-mercapto-1-undecanol (146.3 mmol), DCM (1.56 mol), and pyridine (117.6 mmol) and magnetically stirred for 3 hours at 0 °C. Stirring was continued for another 10 hours at room temperature. Following, the solvent was evaporated using a rotavapor. The residue was diluted in 50 mL of DCM and washed twice with 50 mL of 1N HCl, 1N NaHCO3, and millipore water sequentially. Washed product was dried over Na_2SO_4 for 12 hours. After, the solution was filtered and dried under vacuum yielding to a colourless oil. BBU was characterized by 1H NMR in Chloroform-D (Figure S1). The software ACD/Spectrus by ACD Labs was used to analyse NMR spectra and to determine the purity of the synthesized BBU. Only BBU with more than 80% purity was utilized for ATRP. A Bruker 300 MHz Avance III HD Nano NMR machine was used.

Quartz crystal microbalance with dissipation (QCM-D).

QCM-D measurements were performed on a Q-Sense Explorer microbalance with a single-channel. A 14 mm diameter AT-cut gold-plated quartz crystal with fundamental frequency of 5MHz was used as a sensor. The frequency and dissipation were recorded for seven odd overtones (1^{st}-13^{th}). A temperature ramp of 1°C per minute was programmed for both, increasing, and decreasing of temperatures during phase-transition characterization of the polymer brushes. All the solutions were injected at a constant a flow rate of 50 μl min^{-1}.

The sensors were cleaned after the experiment as per cleaning procedures recommended by the manufacturer [3536]. Briefly, the crystals were exposed to a UV/Ozone treatment for 15

minutes. After, crystals were immersed for 5 minutes into a solution mixture of 5:1:1 volume of millipore water, ammonia (25%) and hydrogen peroxide (30%) preheated to 75°C. Then, crystals were quickly immersed into millipore water and rinsed extensively. Clean crystals were dried with air gas and treated with UV/Ozone for 10 minutes completing the cleaning procedure. Frequency and dissipation initial overtone values were verified to be within the acceptable range specified by the manufacturer.

Initiator assembly.

A monolayer of the BBU initiator was deposited on the surface of a AT-cut gold-plated quartz crystal. BBU assembly process was monitored by QCM-D. First, a baseline was created by flowing through the QCM-D chamber millipore water for at least 10 minutes and until getting a stable baseline. Then, ethyl alcohol was flowed through for at least 10 minutes and until getting a stable frequency signal to normalize for the initiator solvent. Next, 5 mL of a 35 μmol solution of BBU in ethyl alcohol were injected into the QCM-D chamber. After an overnight incubation with BBU solution, the sensor was rinsed by flowing ethyl alcohol for 10 minutes, and Millipore water for another 10 minutes to ensure removal of unattached BBU molecules. The decrease in the frequency from the initial baseline and one obtained during the last rinse with water was used as indicator of BBU attachment to the surface of the QCM-D sensor.

Polymer brush synthesis.

Polymerization was performed using an Atom Transfer Radical Polymerization (ATRP). technique [30]. Polymerization was monitored by QCM-D. Briefly, after BBU deposition on the QCM-D sensor both water and a 3:2 v/v DMF/water solution, were run to be set as solvent baselines. Then, a monomer solution consisting in 4,4′-dinonyl-2,2′-dipyridyl (196.7 μmol), copper chloride (30.3 μmol), and 1 mmol of respective monomer (144, 188 or 300 Da) in 5 mL of degassed 3:2 v/v DMF:water at 60° C was injected into the QCM-chamber. The reaction was allowed for 5 hours. After reaction, the QCM-D chamber was rinsed with 3:2 v/v DMF:water and millipore water respectively. Decrease in the frequency from the initial water baseline to the frequency obtained during the last water rinse elicits the polymer brushes grown over the surface of the sensor. This change in the frequency values were utilized to determine the thickness, and mass of the grafted polymer brushes using Sauerbrey equation [28, 37, 38]. ATRP using QCM-D was carried out for three different molecular weight oligomers of POEGMA: 144, 188, 300 Da.

Polymer brush response to temperature cycles.

Once POEGMA brushes were grafted on the QCM-D sensor, they were subjected to a series of temperature cycles to study their reversible phase transition in millipore water. The temperature of the QCM-D sensor was raised from 24 °C to 65 °C at a 1°C per minute ramp rate, and the temperature was held at 65 °C for 2 minutes to achieve complete collapse of the polymer brushes. Next, the temperature was brought down from 65 °C to 24 °C at a 1°C per minute ramp rate and held at 24°C for 85 minutes to allow for complete re-swelling of the brushes. This process of raising temperature beyond their reported LCST and bringing them back to room temperature (complete collapse and re-swelling) was performed for 10 consecutive cycles controlled by the QSoft 401 software.

Drug loading and release in response to polymer brush phase transition.

Polymer brushes grafted on the surface were tested for its ability to encapsulate and release the drug from the brushes. Brushes are in swollen state at room temperature due to encapsulated water molecules between the brush strands and they squeeze out the water molecules during the change of conformation. This phenomenon was utilized to load the brushes with the model drug known as capsaicin and analyze the release kinetics in response to changing temperatures. The crystal was rinsed with 150 mM sodium chloride solution for at least 10 mins. Capsaicin was dissolved in 0.1 % (of the total volume) of DMSO and the solution was prepared to a final concentration of 0.5 mg mL^{-1} in 150 mM Sodium Chloride solution. Brushes were incubated with the capsaicin solution at least an hour. Following which the brushes were washed with 150 mM sodium chloride solution. The difference in the mass of the brushes before and after capsaicin encapsulation was determined to know the mass of capsaicin encapsulated.

Interpretation of QCM-D data.

Changes in resonance frequency (ΔF) and dissipation (ΔD) were monitored during all the experiments (initiators assembly, polymer growth and temperature transition cycles) at seven odd overtones of fundamental frequency (1^{st}- 13^{th} harmonics). The relationship between frequency changes monitored by QCM-D and mass were calculated using Sauerbrey Equation [37, 38]:

$$m_{QCM-D} = -C\frac{\Delta f_i}{i}$$

with the mass sensitivity constant of the crystal $C = -17.7\ ng\ cm^{-2}\ Hz^{-2}$.

The normalized frequency shifts, $\Delta f = \frac{\Delta f_i}{i}$ of the average frequency changes (harmonics 3–11) were employed to calculate the mass of polymer brushes grafted from the QCM-D quartz sensors. First, third and the last harmonics (F1, D1, F3, D3, F13, and D13) were not considered for further calculations since their generation is related to the unstable edge effects [39, 40]. The ratio of dissipation and normalized frequency shifts, $-\Delta D/\Delta F$, were smaller than 0.2×10^{-6} Hz^{-1}, fulfilling the conditions to use Sauerbrey equation [37]. The thickness of the polymer brushes was calculated by: $d_{QCM} = m_{QCM}/\rho_{brush}$, with ρ_{brush} = 1.08 g cm^{-3} being the density of the solvated polymer film. The thickness obtained was compared between the polymer brushes of different molecular weight. At least three repetitions of polymerizations and phase transition measurements for every MW (144, 188 and 300 Da) of POEGMA were conducted.

Atomic Force Microscopy (AFM).

For AFM measurements, POEGMA-144 and POEGMA-300 brushes were synthesized on 15 mm diameter round coverslips following the same protocols described above but utilizing 2-bromo-2-methylpropionyloxy propyl triethoxysilane as surface grafted initiator (see Supplementary Note). Images were collected in tapping mode with a Veeco (Bruker) Nanoscope Multimode V AFM equipment using MLCT-BIO cantilevers with a nominal

spring constant of 0.6 N m^{-1} and resonant frequency in the range of 90 to 160 kHz (Bruker AFM Probes). All measurements were performed in phosphate buffered saline (PBS, pH 7.4) and temperature was varied from 25 to 60°C using a Thermal Applications Controller (TAC, Bruker).

Bulk Polymerization.

POEGMA polymers were synthesized in bulk to characterize the thermodynamic behaviours of the polymer in solution. Initially, a 3 mL of the thiol initiator (BBU) (85% pure) was added to 25 mL of DMF:water (3:2 v/v) and sonicated for few seconds. 1.32 mol of oligomer was added to the sonicated mixture and was degassed for 10 minutes with N_2. Added 0.004mol of the catalyst copper chloride to the mixture and was set up to heat up to 60°C in an oil bath. Once the solution was heated, 0.23mol of 4,4′-Dinonyl-2,2′-dipyridyl was added and let the contents stir for overnight at 60°C with continuous flush of N_2. After overnight, the mixture was dialyzed in a 3.5KDa Snakeskin dialysis bag in 0.1M KCl solution for a day. The dialysis was continued for another day in 0.01M KCl. At last, the purification was completed by dialyzing in water for two more days. At this point the solution should look cloudy and have no trace of copper chloride. Otherwise, the solution can be passed through a packed alumina column to remove any residues of copper chloride from the reaction. Filtered solution was freeze dried to obtain amorphous bulk POEGMA polymer that was used for experiments. The thermo-responsive attribute of the bulk polymers made of three different molecular weight monomers: 144, 188 and 300Da, were tested by subjecting them to increasing temperatures beyond their LCST temperatures. Changes in the size and conformation of the bulk polymers at the cloud point temperature were studied using Dynamic Light Scattering and UV-Vis spectroscopy [41].

4. Conclusions

Polymers play a significant role in biotechnology as their properties can be engineer for a wide variety of biomedical applications. PEG based thermo-responsive polymers, such as POEGMA are known as ‘smart’ polymers and have drawn attention due to their unique reversible thermodynamic behaviour. Additionally, the biocompatibility nature of PEG analogues such as POEGMA allows for potential applications in the field of nanomedicine. Here, we described QCM-D as a powerful technique to study the thermodynamic behaviour of POEGMA brushes. Using ATRP to synthesize POEGMA brushes from a surface allowed us to grain control over the polymer brushes thickness. The LCST of POEGMA brushes can be directly controlled by proper selection of the monomer molecular weight, which influences the thickness and density of the synthesized polymer brushes. The LCST of POEGMA brushes was determined by following their thermodynamic phase transition by QCM-D and was found to be consistent with the LCST of POEGMA free polymer chains in solution. QCM-D is a powerful technique that allowed us to follow in-situ the thermodynamic phase transition of polymer brushes, which is not possible to achieve by other techniques. It was found that increment in the thickness of POEGMA brushes results in higher LCST. We provided an insight into POEGMA brushes application as biocompatible coatings for controllable and programmable drug delivery. POEGMA brushes can entrap hydrophobic drugs within the polymer chains. When the local temperature

increases beyond the LCST of POEGMA, the polymer brushes collapse releasing the drug. The reversible thermodynamic phase transition of the POEGMA could potentially facilitate multidose drug delivery as POEGMA phase transition is reversible.

Supplementary Material

Refer to Web version on PubMed Central for supplementary material.

Acknowledgements

This work was financially supported by the NIH National Institute of General Medical Sciences (NIGMS), Grant SC1GM130542.

Notes and references

1. Moore TL, Rodriguez-Lorenzo L, Hirsch V, Balog S, Urban D, Jud C, Rothen-Rutishauser B, Lattuada M and Petri-Fink A, Chemical Society Reviews, 2015, 44, 6287–6305. [PubMed: 26056687]
2. Guerrini L, Alvarez-Puebla RA and Pazos-Perez N, Materials, 2018, 11, 1154.
3. Lutz J-F, Journal of Polymer Science Part A: Polymer Chemistry, 2008, 46, 3459–3470.
4. Klok H-A, Journal of Polymer Science Part A: Polymer Chemistry, 2005, 43, 1–17.
5. Bianco-Peled H and Gryc S, Langmuir, 2004, 20, 169–174. [PubMed: 15745016]
6. Ward MA and Georgiou TK, Polymers, 2011, 3, 1215.
7. Jeong B and Gutowska A, Trends in Biotechnology, 2002, 20, 305–311. [PubMed: 12062976]
8. Liu M, Leroux J-C and Gauthier MA, Progress in Polymer Science, 2015, 48, 111–121.
9. Lutz J-F, Akdemir Ö and Hoth A, Journal of the American Chemical Society, 2006, 128, 13046–13047. [PubMed: 17017772]
10. Becer CR, Hahn S, Fijten MWM, Thijs HML, Hoogenboom R and Schubert US, Journal of Polymer Science Part A: Polymer Chemistry, 2008, 46, 7138–7147.
11. Fang Q, Chen T, Zhong Q and Wang J, Macromolecular Research, 2017, 25, 206–213.
12. Roth PJ, Jochum FD, Forst FR, Zentel R and Theato P, Macromolecules, 2010, 43, 4638–4645.
13. Luzon M, Boyer C, Peinado C, Corrales T, Whittaker M, Tao L and Davis TP, Journal of Polymer Science Part A: Polymer Chemistry, 2010, 48, 2783–2792.
14. Yamamoto S-I, Pietrasik J and Matyjaszewski K, Journal of Polymer Science Part A: Polymer Chemistry, 2008, 46, 194–202.
15. Liu M, Leroux J-C and Gauthier MA, Progress in Polymer Science, 2015, 48, 111–121.
16. MILNER ST, Science, 1991, 251, 905–914. [PubMed: 17847384]
17. Slavin S, Soeriyadi AH, Voorhaar L, Whittaker MR, Becer CR, Boyer C, Davis TP and Haddleton DM, Soft Matter, 2012, 8, 118–128.
18. Jonas AM, Glinel K, Oren R, Nysten B and Huck WTS, Macromolecules, 2007, 40, 4403–4405.
19. Laloyaux X, Mathy B, Nysten B and Jonas AM, Langmuir, 2010, 26, 838–847. [PubMed: 19842635]
20. Neugebauer D, Zhang Y, Pakula T, Sheiko SS and Matyjaszewski K, Macromolecules, 2003, 36, 6746–6755.
21. Yamamoto S.-i., Pietrasik J and Matyjaszewski K, Macromolecules, 2007, 40, 9348–9353.
22. Husemann M, Mecerreyes D, Hawker CJ, Hedrick JL, Shah R and Abbott NL, Angewandte Chemie International Edition, 1999, 38, 647–649. [PubMed: 29711554]
23. Kim J-B, Bruening ML and Baker GL, Journal of the American Chemical Society, 2000, 122, 7616–7617.
24. Huang W, Baker GL and Bruening ML, Angewandte Chemie International Edition, 2001, 40, 1510–1512.

25. Moya SE, Brown AA, Azzaroni O and Huck WTS, Macromolecular Rapid Communications, 2005, 26, 1117–1121.
26. Bürgi T, Nanoscale, 2015, 7, 15553–15567. [PubMed: 26360607]
27. Xue Y, Li X, Li H and Zhang W, Nature Communications, 2014, 5, 4348.
28. Yoo S, Kim R, Park J-H and Nam Y, ACS Nano, 2016, 10, 4274–4281. [PubMed: 26960013]
29. Kato M, Kamigaito M, Sawamoto M and Higashimura T, Macromolecules, 1995, 28, 1721–1723.
30. Wang J-S and Matyjaszewski K, Journal of the American Chemical Society, 1995, 117, 5614–5615.
31. Song L, Lin J, Liu P, Li J, Jiang S and Huang D, RSC Advances, 2019, 9, 5540–5549.
32. Liu P, Song L, Li N, Lin J and Huang D, Journal of Thermal Analysis and Calorimetry, 2017, 130, 843–850.
33. Zhang Q, Weber C, Schubert US and Hoogenboom R, Materials Horizons, 2017, 4, 109–116.
34. Jones DM, Brown AA and Huck WTS, Langmuir, 2002, 18, 1265–1269.
35. Harewood K and Wolff JS, Analytical Biochemistry, 1973, 55, 573–581. [PubMed: 4201521]
36. Penfold J, Staples E, Tucker I and Thomas RK, Langmuir, 2002, 18, 5755–5760.
37. Ramos JI and Moya SE, Macromolecular Chemistry and Physics, 2012, 213, 549–556.
38. Sauerbrey G, Zeitschrift für Physik, 1959, 155, 206–222.
39. Hsia C-Y, Chen L, Singh RR, DeLisa MP and Daniel S, Scientific reports, 2016, 6, 32715–32715. [PubMed: 27600663]
40. Mechler A, Praporski S, Atmuri K, Boland M, Separovic F and Martin LL, Biophys J, 2007, 93, 3907–3916. [PubMed: 17704161]
41. Joh DY, McGuire F, Abedini-Nassab R, Andrews JB, Achar RK, Zimmers Z, Mozhdehi D, Blair R, Albarghouthi F, Oles W, Richter J, Fontes CM, Hucknall AM, Yellen BB, Franklin AD and Chilkoti A, ACS Applied Materials & Interfaces, 2017, 9, 5522–5529. [PubMed: 28117566]

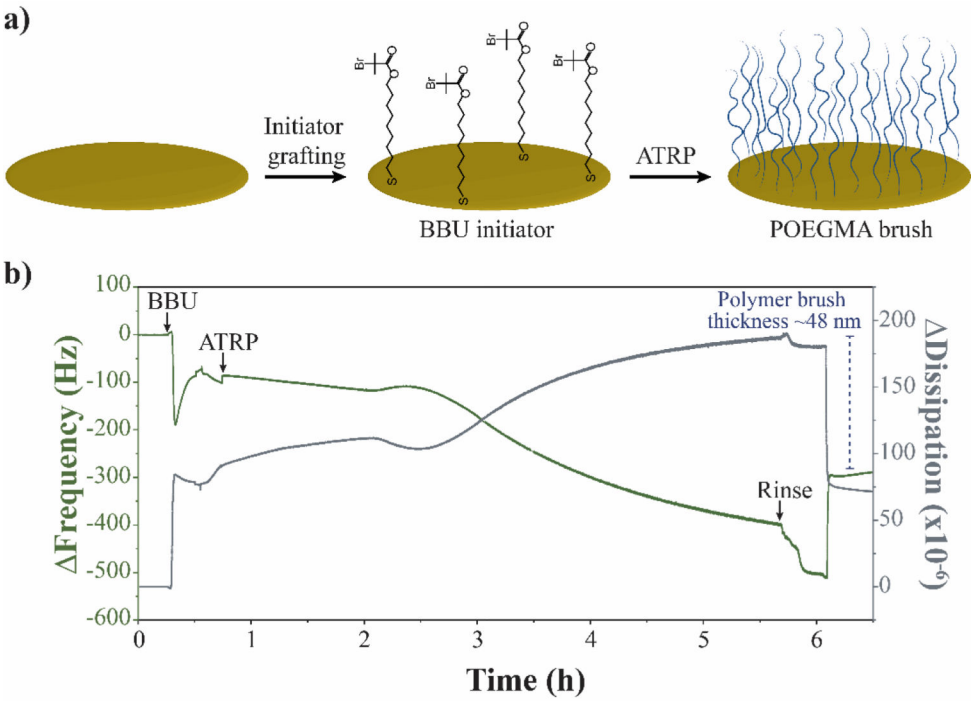

Figure 1.

POEGMA brushes synthesis. a) Schematic illustration of the in-situ grafting of polymer brushes over a QCM-D sensor. b) QCM-D graph following POEGMA-144 brushes synthesis through ATRP. Monitoring of ΔFrequency is indicated in green, ΔDissipation in grey and the difference in ΔFrequency used to calculate polymer thickness in blue.

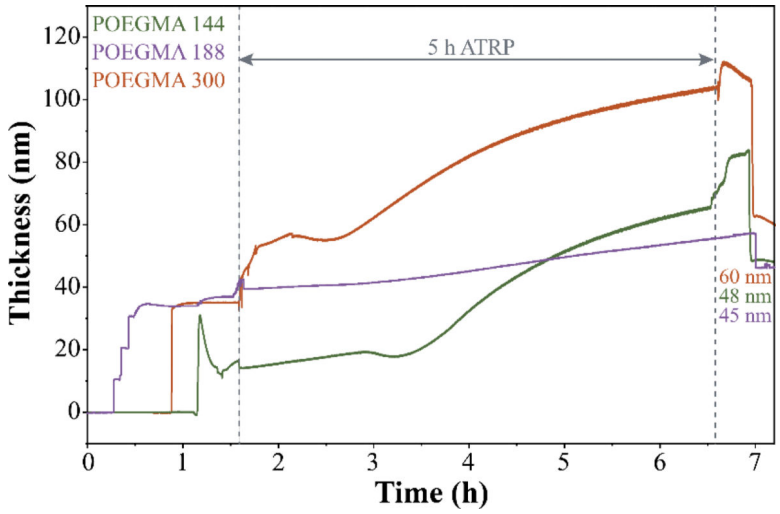

Figure 2.

Growth of POEGMA brushes during ATRP. Thickness of POEGMA brushes synthesized in-situ from a gold-plated quartz QCM-D sensor using three monomers with different molecular weight: 144 g mol^{-1} (POEGMA-144, green), 188 g mol^{-1} (POEGMA-188, purple), and 300 g mol^{-1} (POEGMA-300, orange).

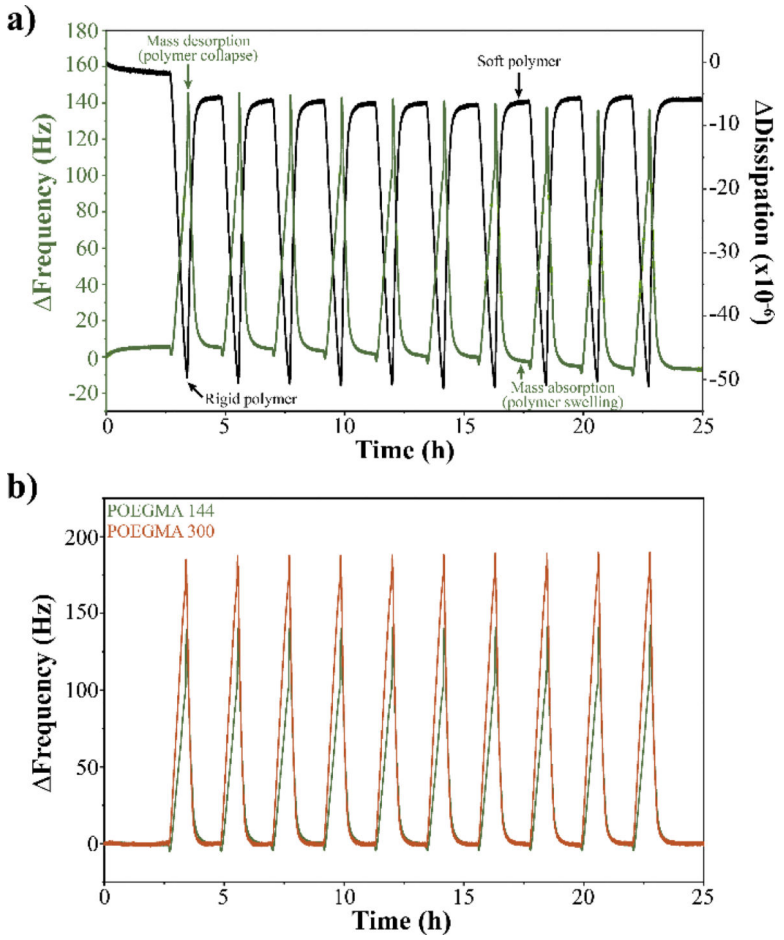

Figure 3.

Thermodynamic phase transition of POEGMA brushes followed by QCM-D. a) Phase transition graph of POEGMA-144 brushes when subjected to 10 consecutive temperature cycles from 24°C to 65°C. Increase in the frequency is accompanied by a decrease in the dissipation, indicating mass desorption and the formation of a stiffer coating when the polymer collapses as temperature increases. Decrease in the frequency is accompanied by an increase in the dissipation, indicating mass absorption and the formation of a softer coating as consequence of polymer swelling when the temperature decreases below the LCST. b) Phase transitions of POEGMA-144 (green) and POEGMA-300 (orange) brushes.

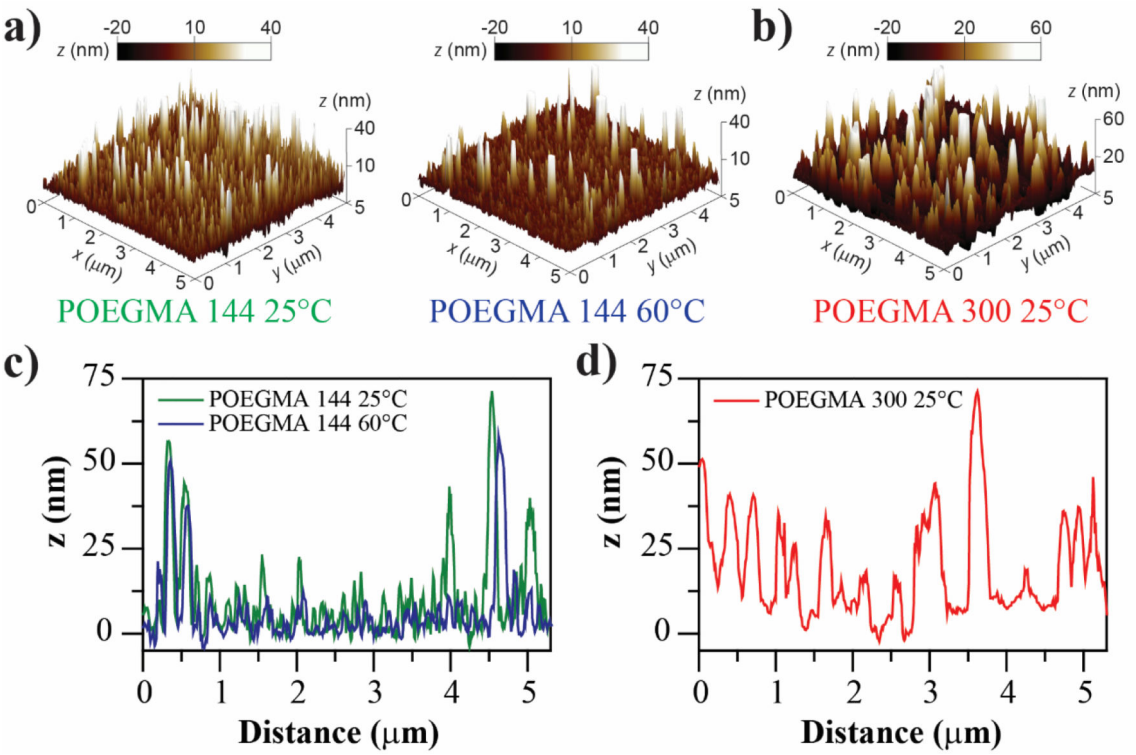

Figure 4.

POEGMA brushes topography studied by AFM. a) AFM three-dimensional height images of POEGMA-144 at 25°C and 60 °C. The same area of the sample was scanned at both temperatures. The collapse of polymer brushes above the LCST is inferred from the height decrease of peaks and structures. b) AFM three-dimensional height image of POEGMA-300 at 25°C. Higher peaks and structures are observed in comparison with POEGMA-144. c) Height profiles of POEGMA-144 at 25°C and 60°C.

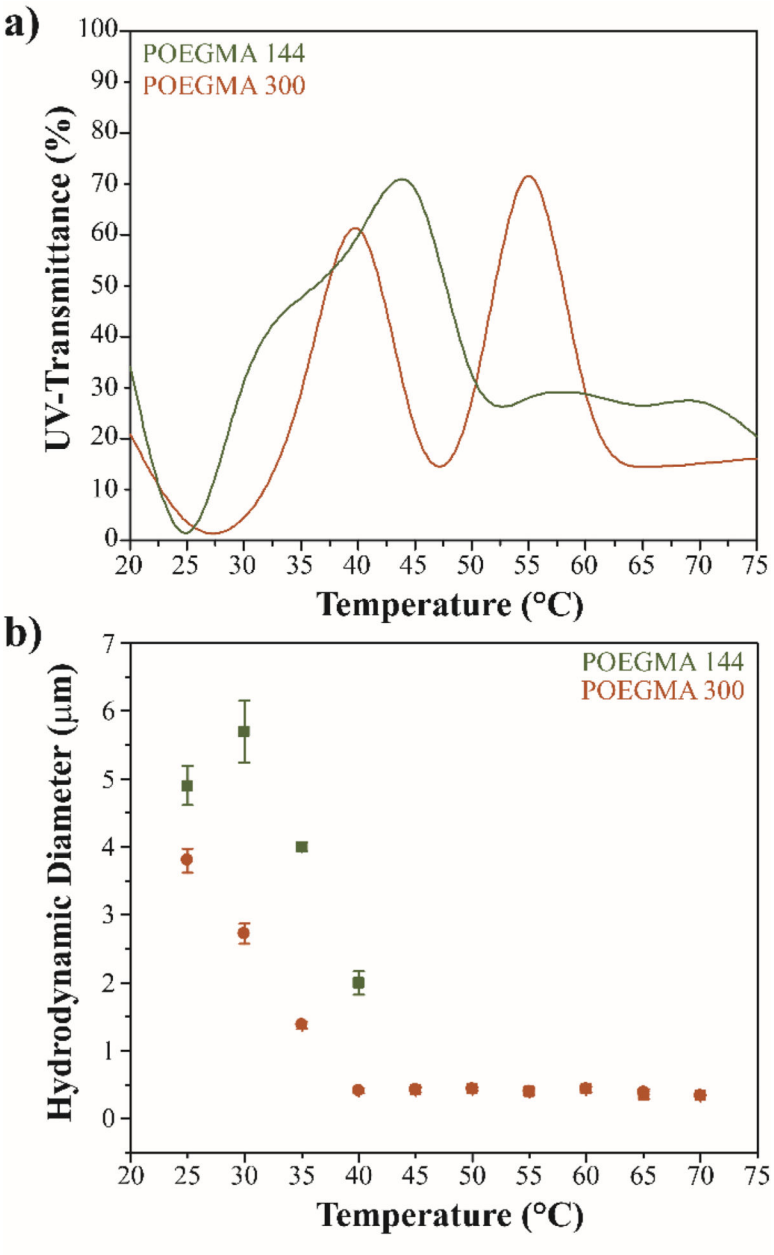

Figure 5.

Thermodynamic phase transition of free POEGMA polymer chains in solution. a) UV-Transmittance of the polymer in solution as temperature increases. b) Hydrodynamic diameter of polymer in solution at different temperatures.

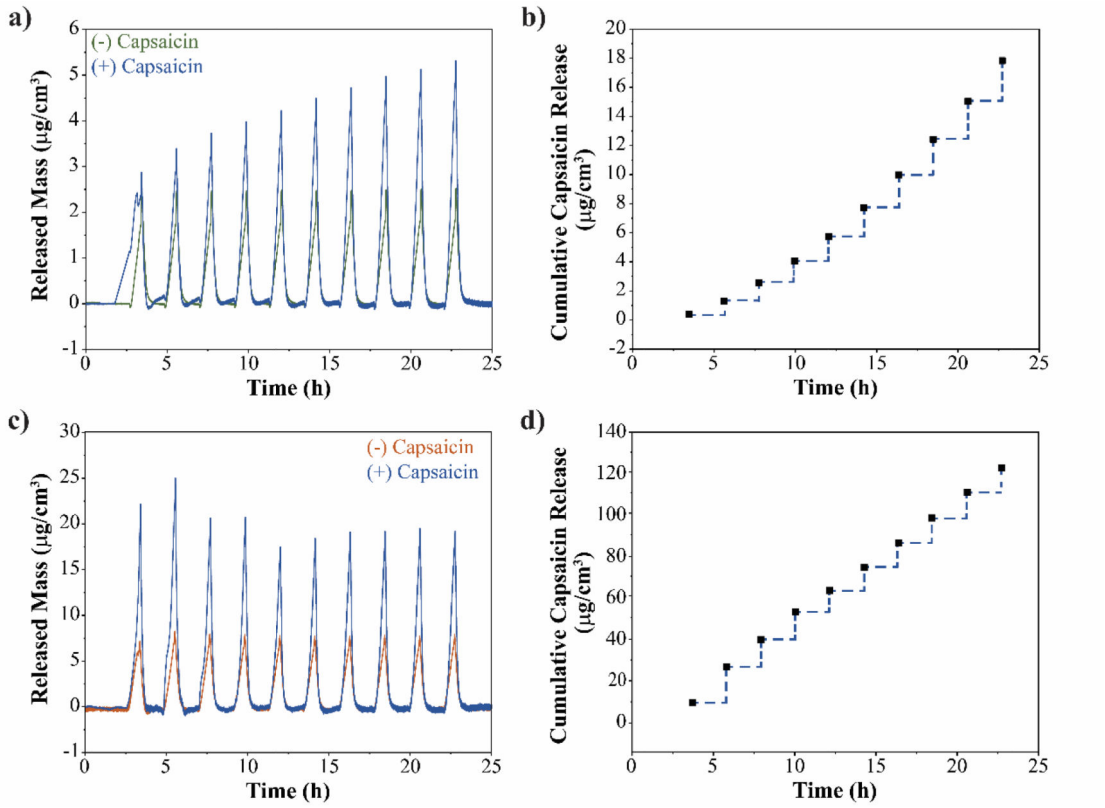

Figure 6.

Capsaicin release from POEGMA brushes triggered by local increase of temperature. a) Mass released over time from POEGMA-144 brushes loaded (blue) and unloaded (green) with capsaicin during 10 temperature cycles. b) Cumulative capsaicin release profile from POEGMA-144 brushes triggered by the local increase of temperature. c) Mass released over time from POEGMA-300 brushes loaded (blue) and unloaded (orange) with capsaicin during 10 temperature cycles. b) Cumulative capsaicin release profile from POEGMA-300 brushes triggered by the local increase of temperature.

Table 1.

Summary of the properties of the different POEGMA brushes synthesized from the surface of a QCM-D sensor. ΔFrequency (Hz) was used to calculate mass (μg cm^{-2}) using Sauerbrey equation. Thickness (nm) was obtained from calculated mass and polymer density.

Polymer	ΔFrequency (Hz)	Mass density (μg cm^{-2})	Thickness
POEGMA-144	−296 ± 33	5.2 ± 0.6	48.5 ± 5.4
POEGMA-188	−307 ± 188	5.4 ± 3.3	50.3 ± 30.8
POEGMA-300	−417 ± 49	7.4 ± 0.9	68.4 ± 7.9